Int j simul model 22 (2023) 4, 619-630
Original scientific paper

DESIGN AND MOTION SIMULATION OF CONVEYOR PRODUCTION LINE FOR SALTED KELP TURNOVER BOX

Zhang, W.[#]; Zhang, C. T. & Deng, C. H.
Rongcheng College, Harbin University of Science and Technology, Weihai, 264300, China
E-Mail: zhangwei8171@hrbust.edu.cn ([#] Corresponding author)

Abstract
To improve the automation degree of kelp turnover box conveying, a conveyor production line of salted kelp turnover boxes was developed, and a motion simulation model of the production line was designed. The conveyor production line was composed of a colour recognition system, an online weighing system, and a sorting and conveying system. After parametric design and model assembly, a motion simulation model of the conveyor production line was established. Based on the ADAMS solver built in UG software, the sorting action simulation, motion characteristic analysis, and working process simulation of differently coloured turnover boxes were performed using the STEP motion function, and the accuracy of the system structure and model was verified by simulation. Results showed the STEP motion function can control the time period driven by the model and obtain the motion change law of the turnover box in different time periods. The motion displacement and speed of the cylinder push rod changed smoothly with time, which is consistent with the actual situation real-world problems and advance the knowledge and practice of simulation.
(Received in June 2023, accepted in October 2023. This paper was with the authors 1 month for 2 revisions.)

Key Words: Turnover box, Motion simulation, Motion function, ADAMS

1. INTRODUCTION

Kelp, a kind of dark brown marine algae, is a type of food with unique flavour, soft taste, and rich nutrition, which is suitable for the young and old. Daily eaten kelps are mostly salted kelp products, that is, the harvested kelps are hot-cooked, cooled, stirred with salt, and then salted, followed by processing into all kinds of products such as shredded kelps, kelp cubes, and kelp knots. Salted kelps, which are about 1.5–1.8 m in length, are manually cut into 3–4 segments and stored in turnover boxes, which are then conveyed to the processing positions of shredded kelps, kelp cubes, and kelp knots manually or by forklifts. At each processing position, the salted kelps of about 0.4–0.5 m in length are processed into shredded kelps, kelp cubes, and kelp knots.

Manual or forklift-aided conveying of salted kelp turnover boxes is characterized by low production efficiency, high labour costs, and a low degree of automation. Developing the conveyor production line of salted kelp turnover boxes is important to improving the automation and intelligence levels of production and realizing the automatic sorting and conveying of salted kelp turnover boxes [1-2]. The development of the conveyor production line includes theoretical calculation, mechanism design, and system control, in which many factors are involved with great technical difficulties. Meanwhile, this brings about enormous challenges to the research on the conveyor production line of salted kelp turnover boxes.

On this basis, scholars have extensively explored the structural composition, conveying method, and sorting method of the conveyor production line of salted kelp turnover boxes [3-8]. However, a large amount of theoretical analyses and calculations are still required for the structural design and kinematic analysis, accompanied by deviation from the actual working status in aspects of the assembly relationship and motion coupling of each component in the production line. Therefore, to simulate accurately whether components in the production line interfere with one another and present a motion coupling state, set a motion driving function to control the motion law of each component in the production line, analyse the motion simulation

results through intuitive model animation and parametric curve changes, and carry out an optimization design are urgent.

Therefore, this study designs a kind of conveyor production line of salted kelp turnover box, establishes the movement simulation model of the conveyor production line through the UG/Motion analysis module and the STEP motion function, and simulates the sorting action, motion characteristics, and working process of turnover boxes with different colours, aiming at more accurately predicting the movement change law of turnover boxes in different time periods, and then providing reference for the construction and performance evaluation of the conveyor production line system of salted kelp turnover box.

2. STATE OF THE ART

At present, scholars have conducted much work on the motion simulation of mechanical mechanisms or system devices. Based on ADAMS and MATLAB software, Sosa-Mendez et al. [9] performed kinematics, dynamics, and motion control co-simulation of the Stewart–Gough platform, providing a new method for the application of parallel robots, but restricted to single-platform research. Arreguin et al. [10] introduced a design and simulation method for a parallel kinematic (PK) testbed applied to head impact. This testbed was used to provide motion to a head mannequin to impact against a steel plate in different directions, and ADAMS software was used for modelling and motion simulation. The analysis results showed the PK testbed scheme is feasible, and the PK testbed can generate an acceleration of 50 g on the head's centre of mass under lateral impact conditions, but it only simulates the head hitting the steel plate. Nidhi et al. [11] studied the bio-inspired skeletal model construction and kinematic analysis of humanoid spine and ribs and used a three-segment hyper redundant mechanism to imitate the human mimetic spine. A systematic CAD model based on this algorithm was developed, and motion simulation analysis was carried out by ADAMS software. The simulation results were very consistent with the human motion range, but the motion speed and acceleration were not analysed. Amiri et al. [12] studied the optimization and control of an energy-efficient vibration-driven robot. For the two-module vibration-driven robot, first, the control dynamic equation of the robot was deduced and solved by using MATLAB/Simulink technology, and then the obtained results were compared with the MSC Adams simulation results, thus verifying the correctness of the dynamic model of the robot, but the motion simulation of multiple robots was not carried out. Cretescu et al. [13] analysed the dynamic characteristics of a Delta parallel robot with flexible links and joint clearances and highlighted the influence on the dynamic behaviour of the Delta robot by considering the individual and combined effects of clearances and friction in the spherical joints as well as the flexibility of the rod elements. The CAD modelling of the Delta robot and its motion simulation on a representative spatial trajectory, where the maximum allowed values of speed and acceleration were reached, were performed using CATIA and ADAMS software packages, but only the spatial trajectory of a single parallel robot was analysed. John et al. [14] carried out numerical investigations, development, and control of a Cartesian (3-PRRR) parallel manipulator and focused on the development of a Cartesian parallel manipulator (CPM) with multiple limb assembly configurations. An optimal configuration of the 3-PRRR CPM was identified after analysing the interference-free workspace of various limb assembly conditions, and the Euler–Lagrange dynamic modelling of the CPM was validated by using ADAMS software, but detailed research and analysis of the motion co-simulation of multiple (sets) of such parallel robots were lacking. Satpute et al. [15] carried out the design and analysis of motion- and energy-regulating vibration harvester and proposed a novel design of energy harvester, which converts harmonic or random vibration energy into useful electric power. The energy harvester comprises a mechanical motion rectifier, a motion regulator, a strain energy storage element,

and a rotary electric generator. Rigid body simulations in ADAMS and MATLAB were used in the design and analysis of the energy harvester with investigations into the effect of remarkable design parameters. However, the content of motion simulation analysis was simple, and motion parameters such as displacement and speed were analysed in detail. Boomeri and Tourajizadeh [16] designed, modelled, and controlled a grip-based climbing robot, which consists of a triangular chassis and three actuating legs, and its related kinematic and kinetic models were developed. Robot modelling was investigated for two different modes, namely, climbing and manipulating phases. Considering the redundancy of the proposed robot and the parallel mechanism employed in it, the active joints were selected properly, and its path was planned to accomplish the required missions Finally, MATLAB and ADAMS software were used for simulation, which verified the correctness of the modelling, but the motion simulation of the climbing robot in different stages was not controlled by motion functions. Thomas et al. [17] analysed the kinematics and dynamics of a 3-PRUS spatial parallel manipulator. The kinematic equations for the proposed spatial parallel mechanism were formulated using the Modified Denavit–Hartenberg technique considering active and passive joints. The analytical model of the robot dynamics was presented using the Euler–Lagrangian approach with Lagrangian multipliers to include the system constraints, and the analytical results of the dynamic model were compared with the ADAMS simulation results for a predefined trajectory of the end effector, but the structural optimization and multirobot motion simulation of parallel robot were not studied in detail. Karamipour et al. [18] carried out conceptual design, motion equation construction, and motion simulation analysis for the reconfigurable mobile robot with adjustable width and length. Considering the motion restrictions existing in conventional wheels, omnidirectional wheels are used in robot structure, accordingly, the robot was able to move in the direction of wheels' axis. Using ADAMS software, the designed robot structure was simulated and compared with the derived motion equation. The results showed the system structure was feasible. The calculated energy consumption in a robot that used transverse adjustment to cross obstacles decreased by 12 % compared with a robot that climbed the obstacle and decreased by 10 % compared with the path planning method, but the motion function was not adopted for control in different motion stages. Chen et al. [19] established a 3D model of the working device of the log grab in UG software, established a motion simulation model, defined its link and joint, designed a reasonable drive based on the STEP function, then set up a simulation scheme, and obtained the animation and simulation results by solving. The results showed the structural design of the working device of the log grab could meet the design requirements. Nevertheless, the co-simulation of the log grab and supporting equipment was not carried out. Liu et al. [20] studied the motion simulation of the virtual model of the embossing machine based on ADAMS software, analysed the structure of the embossing machine, imported the established 3D model of the embossing machine into ADAM, and set relevant parameters and relevant joints to carry out simulation and motion analysis, which provided data analysis for the concave–convex roller of the embossing machine in the variable speed state and the uniform speed state, but no motion function was used to carry out motion simulation under different modes. Taking the picking mechanism of a rocker-type mulberry leaf picker as the main study object, Liu et al. [21] conducted kinematic and dynamic simulation analysis of the mechanism and compared the theoretical motion calculation results with the simulation analysis results, but they did not simulate the real working status of the mulberry leaf picking machine and surrounding equipment. Zhao et al. [22] studied the modelling and kinematics of globoidal indexing cam mechanism and analysed the influences of the angular velocity and angular acceleration curve oscillation of the mechanism and their causes through ADAMS kinematic simulation. Ma et al. [23] simulated and analysed the motion of a fruit picking manipulator based on ADAMS software. By calculating the motion driving function of each hydraulic cylinder, a group of picking actions of the manipulator was simulated, and the

stress change curves of several key joints on the manipulator were obtained. Liu et al. [24] conducted motion simulation analysis of a picking mechanical arm for fruit trees via ADAMS, simulated a group of picking motions of the mechanical arm by calculating the motion driving function of each hydraulic cylinder, and obtained the stress change curves of several key joints on the mechanical arm. The simulation results showed the gait characteristics of the lower limb prosthesis had good bionic properties driven by the joint angle curve.

The above studies were mainly aimed at the motion simulation of a single piece of equipment or the simulation of the key structures and key actions of a piece of equipment, while the co-simulation with surrounding supporting equipment was not considered, not to mention the motion simulation study on a production line or even the relevant study on the application of the STEP motion function in the motion simulation of production lines. In this study, a motion simulation model of a conveyor production line is constructed with the conveyor production line for salted kelp turnover boxes as the study object. Then, links and joints are created, the motion driver is defined through the STEP motion function, and the motion simulation of the production line is calculated using the built-in ADAMS/Solver of UG. On this basis, the motion simulation of the conveyor production line is obtained, and the change laws of motion parameters such as the displacement and velocity of salted kelp turnover boxes in different periods are acquired, providing a basis for optimizing and testing the conveyor production line of salted kelp turnover boxes.

The remainder of this study is organized as follows: In Section 3, the system structure of the kelp turnover box conveyor production line is described, a simulation model of the conveyor production line is established, and a motion analysis scheme and a solving algorithm of the conveyor production line are constructed. In Section 4, the sorting action simulation, motion characteristic analysis, and working process simulation of differently coloured turnover boxes are conducted through calculations, thus obtaining the motion change laws of turnover boxes in different periods and the motion characteristics of cylinder push rods. In the final section, the whole studies are summarized, and relevant conclusions are presented.

3. METHODOLOGY

3.1 Design of the kelp turnover box conveyor production line system

The conveying line of kelp turnover boxes was mainly composed of a colour recognition system, an online weighing system, and a sorting conveying system, all of which worked together to complete the conveying and sorting of kelp turnover boxes, as shown in Fig. 1. The colour recognition system was used for colour recognition and counting the number of turnover boxes, and a colour recognition sensor was installed on it. The turnover boxes were red, blue, and green, which were used to store the head, middle, and tail of the cut-salted kelps.

When placed into the conveyor, differently coloured turnover boxes first entered the colour recognition area, the colour recognition sensor was responsible for the real-time detection of the colour of turnover boxes, and online weighing was performed through the weighing system. In this case, only one turnover box should be in the weighing area. When the turnover box arrived at the sorting and conveying system, the side-pushing cylinder completed the corresponding action by controlling the system-detected colour signal of the turnover box, the red and green turnover boxes were pushed into the bilateral subconveyors, and the blue turnover box continued conveying on the main conveyor, thus realizing the sorting of turnover boxes.

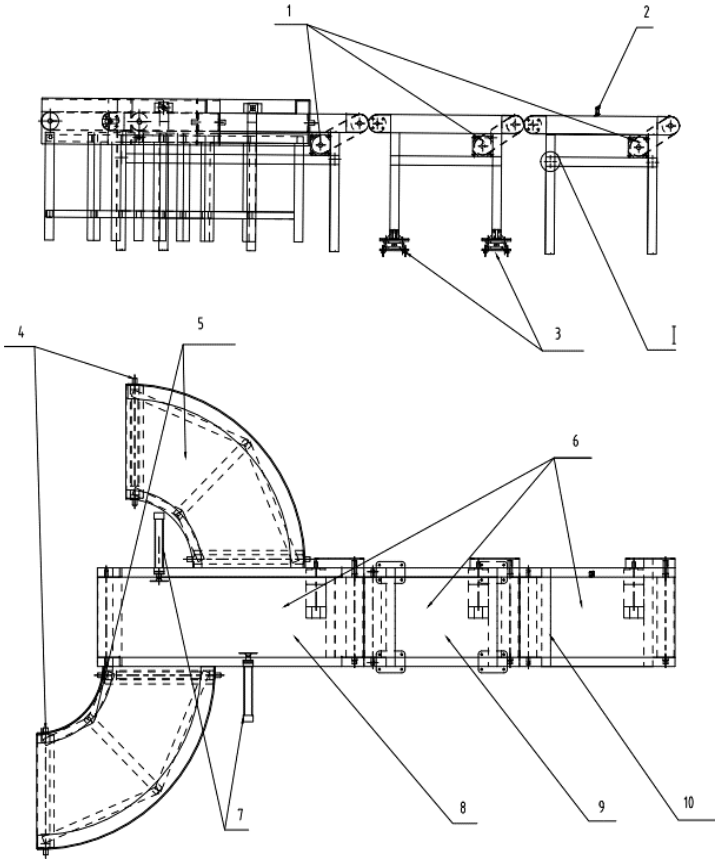

Tags (1 to 10):
1. Variable frequency motor
2. Colour recognition sensor
3. Weighing sensor
4. Roller
5. Subconveyor
6. Main conveyor
7. Side-pushing cylinder
8. Sorting and conveying system
9. Online weighing system
10. Colour recognition system

Figure 1: Composition of conveyor production line.

3.2 Simulation modelling for the kelp turnover box conveyor line

The interference of the system mechanism was analysed using the UG motion simulation module. The gauge point on the link in the mechanism or the displacement, velocity, and acceleration of the joints was analysed, and the actual motion of the mechanism was simulated using charts or animations. Next, all mechanisms or parts and components of the conveyor line were subjected to 3D modelling, followed by system assembly in the assembly module, as shown in Fig. 2.

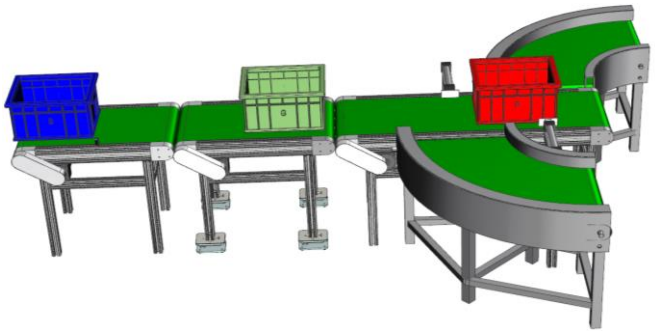

Figure 2: Assembly of the conveyor production line.

3.3 Motion simulation analysis scheme

The mechanism of the kelp turnover box conveyor line system was complex, and the creation of a motion analysis scheme was the key to motion simulation. The motion analysis module automatically copied the assembly files of the main model and established a series of different motion analysis schemes, including creating links, creating joints, and defining motion drivers.

Creation of links: Links represent moving parts in the system mechanism, and all moving parts must be created as links. The creation of links includes defining link object, mass attribute, initial rotational velocity, and movement speed, 17 links were defined.

Creation of joints: The joints connected the links in the system mechanism so that the links moved in an orderly manner. A total of 17 joints were created, including 7 sliding pairs, 2 planar pairs, 2 cylindrical pairs, and 6 revolute pairs.

Defining of motion drivers: Motion drivers were parameters assigned on the joints to control the motion, mainly including five types: non drive, constant drive, simple harmonic motion drive, motion function, and joint motion drive. In this study, constant drive and motion function (STEP) function were mainly used for motion simulation.

The STEP function is mathematically expressed as follows:

$$step(x, x_0, h_0, x_1, h_1) = \begin{cases} h_0, & x \le x_0 \\ h_0 + x - x_0 x_1 - 2x_0 h_1 - h_0, & x_0 < x < x_1 \\ h_1, & x \ge x_1 \end{cases} \quad (1)$$

where x is the independent variable; h denotes the function value; x_0 and x_1 stand for the initial value and the ending value of the independent variable, respectively; h_0 and h_1 are the initial value and the ending value of the STEP function, respectively. Within the time period of x_0–x_1, the function changes from h_0 to h_1 approximately to a quadratic function. In general, the STEP function is expressed in two forms, and one is the nested form, as shown below:

$$step(x, x_0, h_0, x_1, step(x, x_2, h_2, x_3, step(x, x_4, h_4, x_5, h_5))) \quad (2)$$

The other is superposition with the following function expression:

$$step(x, x_0, h_0, x_1, h_1) + step(x, x_2, 0, x_3, h_3) + step(x, x_4, 0, x_5, h_5) \quad (3)$$

In this motion simulation analysis, the lateral sorting motion of the cylinder push rod and push plate is realized through the superposed STEP function, and the STEP function drive acts on the sliding pair of two cylinder push rods and push plates. The STEP function of the push rod and push plate of cylinder 1 is as follows:

$$step(x, 8.55, 0, 8.75, 160) + step(x, 10, 0, 11, -160) \quad (4)$$

The STEP function of the push rod and push plate of cylinder 2 is as follows:

$$step(x, 0.55, 0, 0.75, 160) + step(x, 1.5, 0, 2.5, -160) \quad (5)$$

3.4 Motion simulation calculation and solving algorithm

The UG motion simulation was calculated and solved by ADAMS/Solver, and the creation of a motion analysis scheme was the preprocessing stage of the whole analysis. According to the information of the analysis scheme, the internal ADMAS data file was generated and then sent to the ADAMS solver for solving. The solving function of ADAMS/Solver is as follows:

Selection of generalized coordinates: ADAMS uses the Cartesian coordinates of the centre of mass of the rigid body and the Euler angle reflecting the orientation of the rigid body as generalized coordinates, $q_i = [x, y, z, \psi, \theta, \varphi]_i^T$ and $q = [q_1^T, q_2^T, \cdots, q_n^T]^T$, namely, each rigid body is described by six generalized coordinates. Because non-independent coordinates are adopted, the number of system dynamics equation sets is the largest, and this is a highly sparsely coupled differential-algebraic equation, which can be efficiently solved through the sparse matrix method.

Establishment of the kinematic equation: A system motion equation is established through the Lagrangian multiplier method:

$$\frac{d}{dt}\left(\frac{\partial t}{\partial q}\right)^T - \left(\frac{\partial t}{\partial q}\right)^T + f_q^T \rho + g_q^T \mu = Q \tag{6}$$

In case of a holonomic constraint equation:

$$f(q,t) = 0 \tag{7}$$

In case of a nonholonomic constraint equation:

$$g(q,\dot{q}t) = 0 \tag{8}$$

where T is the kinetic energy of the system, Q is the generalized force matrix of the system, ρ stands for a Laplace multiplier array corresponding to holonomic constraints, μ is a Laplace multiplier array corresponding to nonholonomic constraints, q is the generalized coordinate array of the system, and $\dot{q}$ is the generalized velocity array of the system.

Solving algorithm: Two algorithms can be used in system analysis and calculation:

(1) Three powerful integral solving programs with variable order and variable step size, DSTIFF integrator, BDF integrator, and GS-TIFF integrator, are used to solve sparsely coupled nonlinear differential-algebraic equations and are applicable to the simulation of rigid systems.

(2) The ABAM integral solving program uses the coordinate separation algorithm to solve the differential equation of independent coordinates and is suitable for simulating the systems whose replicated eigenvalue experiences sudden changes or radio frequency systems.

4. RESULT ANALYSIS AND DISCUSSION

Before kinematic simulation and analysis, a resolving scheme was set up, and two parameters, namely, simulation time and steps, were defined. The resolving scheme time of turnover boxes on the conveyor line was set to 10 s, in which the conveying of one turnover box was rightly completed. In addition, the number of steps was set to 100, and the step size was 0.1. After resolving analysis was completed, the motion simulation of the system mechanism could be represented in the form of an animation. Subsequently, the motion analysis data were output in the form of tables or charts through the chart function provided by the UG motion simulation postprocessing module. A gauge point was made at the front end of blue, green, and red turnover boxes (namely gauge points A001, A002, and A003, respectively) to observe the motion trajectory, displacement, and velocity of turnover boxes conveniently.

Through the STEP function-based motion control of the conveyor production line, the production line could move as required, and whether it could reach the action requirements and experienced collision should be determined through interference checking. Interference checking is the most effective means of evaluating virtual assemblies. Whether the system design is reasonable can be evaluated through interference checking of the virtual assembly of the conveyor production line to provide early-stage verification for the subsequent motion simulation. In this study, the already assembled production line was subjected to the interference checking using the analysis function of UG. No interference phenomenon was found in the assembly, indicating reasonable production line assembly and proving each part and component met the design requirements and would not affect the overall coordination of the system motion.

Fig. 3 shows the effect diagram of the conveyor production line at different times after the simulation analysis. The red turnover box was conveyed to the left by the push rod of cylinder 2 upon reaching this cylinder. The green turnover box moved along the main conveyor and kept moving forward without changing direction. Upon reaching cylinder 1, the blue turnover box was conveyed to the right under the action of the push rod of cylinder 1. The motion trajectories of the three turnover boxes were consistent with the actual production.

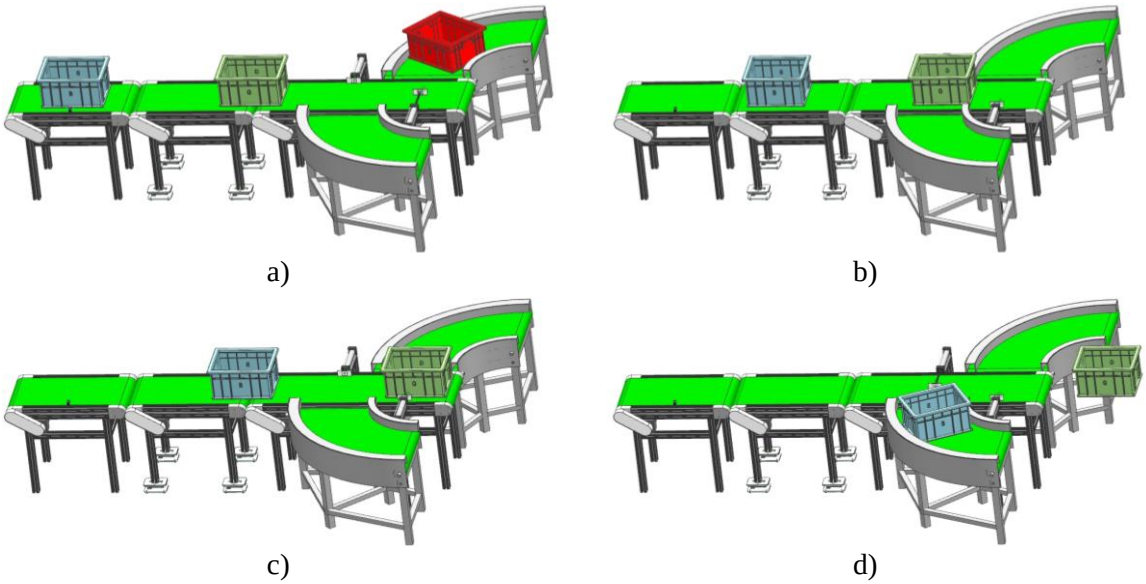

a) b) c) d)

Figure 3: Motion simulation effect of the conveyor production line.

Figs. 4 and 5 show the displacement–time diagram and the speed–time diagram of the turnover boxes, respectively. The Y-direction displacement increment of the green turnover box in the middle was 0, and it performed a uniform linear motion at about 200 mm/s. The Y-direction displacement increment of the blue turnover box was constant at first and then increased, that is, it moved linearly at a constant speed and then moved at a variable speed along the lateral conveyor under the action of the side-pushing cylinder. The initial position of the red turnover box was close to the right side of the production line, and the linear uniform distance was short. Then, under the action of the side-pushing cylinder, the red turnover box moved at a variable speed along the lateral conveyor.

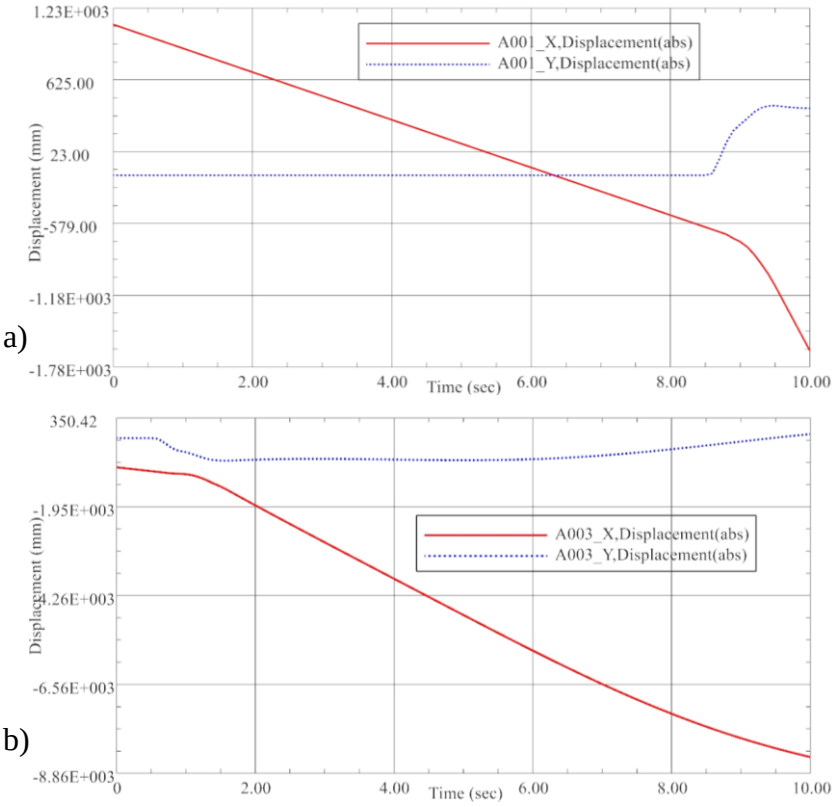

Figure 4: Displacement–time diagram of turnover boxes.

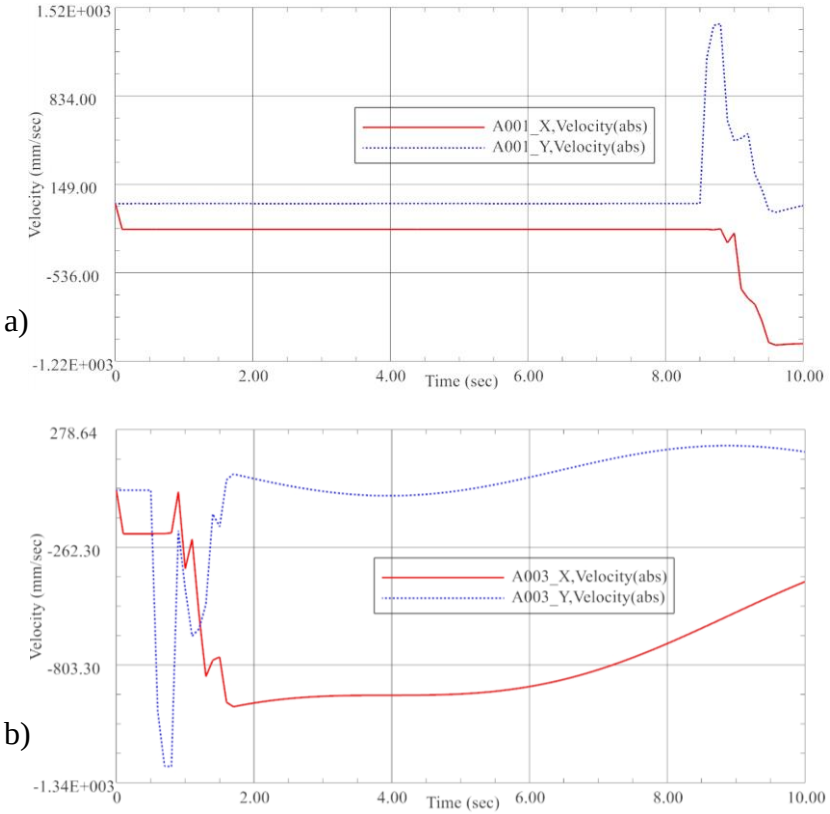

Figure 5: Speed–time diagram of turnover boxes.

The time-dependent change curves of the motion displacement and speed of the cylinder push rod are displayed in Figs. 6 and 7, respectively.

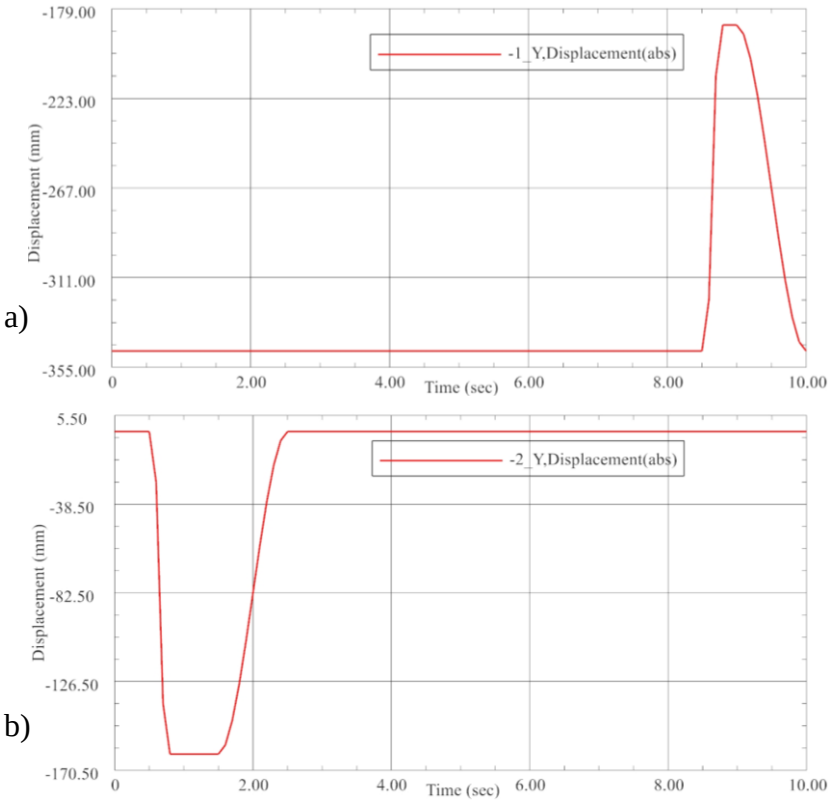

Figure 6: Displacement–time diagram of the cylinder push rod.

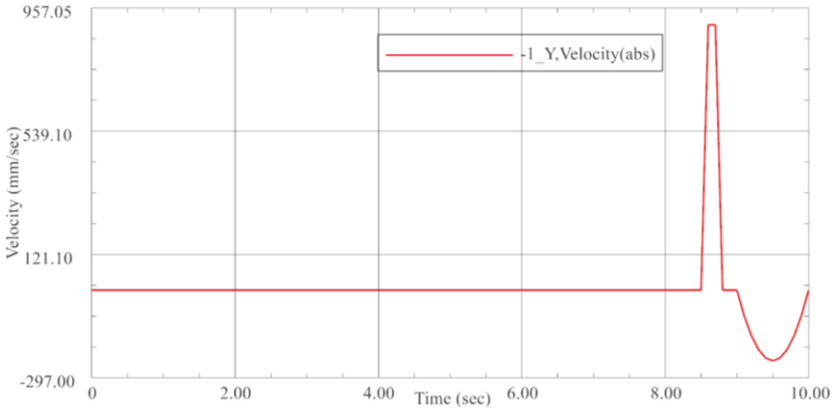

Figure 7: Speed–time diagram of the cylinder push rod 1.

Table I shows the speed change of the cylinder push rod 1, Upon the contact of the cylinder push rod with turnover box, the speed was the highest, approaching 900 mm/s. Afterward, the speed gradually decelerated under the gravitational resistance of the turnover box, and the variation trend was gentle without fluctuations, which was in line with the actual situation and met the basic requirements for the continuity and stationarity of the planned path for the cylinder push rod. Moreover, the reasonability of system kinematic parameters was ensured, and the correctness of STEP function settings was verified by the simulation results.

Table I: Speed change of the cylinder push rod 1.

Time step	**Time** (s)	**Speed** (mm/s)
78	7.8	0
80	8.0	0
82	8.2	0
84	8.4	0
86	8.6	900
88	8.8	0
90	9.0	0
92	9.2	-153.6
94	9.4	-230.4
96	9.6	-230.4
98	9.8	-153.6
100	10.0	0

5. CONCLUSION

To improve the automation degree of kelp turnover box conveying, reduce the labour intensity, and explore the motion characteristics of the turnover box conveyor system, a salted kelp turnover box conveyor production line was developed in this study. Then, a motion simulation model of the production line was designed, and simulation and theoretical analysis were combined to simulate and analyse the motion of the conveyor production line. Finally, the following conclusions could be drawn:

(1) The established STEP motion function is accurate and can truly simulate the sorting action and motion characteristics of turnover boxes.

(2) The structure of the side-pushing cylinder is reasonable, and the variation law of the motion parameters of the cylinder push rod is consistent with the actual situation. The motion simulation of the conveyor production line runs smoothly.

With simulation and theoretical study combined, the analysis for the motion simulation of the conveyor production line was proposed in this study, and the established motion simulation

model and solving algorithm for the conveyor production line of salted kelp turnover boxes approximated the reality of production sites, being of certain reference importance for the follow-up development of the conveyor production line of salted kelp turnover boxes.

ACKNOWLEDGEMENT

The study was supported by the Science and Technology Enterprise Innovation Ability Promotion Project of Shandong Province in China (No. 2021TSGC1319).

REFERENCES

[1] Zhao, Y.-L.; Zhao, Q.; Li, Z.-Q. (2023). Research on control system of carya cathayensis shell breaking automatic production line based on PLC, *Food & Machinery*, Vol. 2023, No. 1, 111-115, doi:10.13652/j.spjx.1003.5788.2022.60101

[2] Gui, A.-H.; Ye, F.; Gong, Z.-M.; Gao, S.-W.; Liu, P.-P.; Wang, S.-P.; Zheng, P.-C.; Teng, J.; Wang, X.-P.; Zheng, L.; Feng, L. (2021). Optimization of key processing technology of flat green, *Food Research and Development*, Vol. 42, No. 6, 49-56

[3] Xu, N.; Hou, X. Y.; Jia, N. (2022). Optimization of multi-stage production scheduling of automated production, *International Journal of Simulation Modelling*, Vol. 21, No. 1, 160-171, doi:10.2507/IJSIMM21-1-CO3

[4] Shen, N. Y.; Wu, X.; Li, J.; Su, K.; Zhu, G. S. (2020). Research on pre-maintenance strategy of key equipment in automatic production line, *Journal of Mechanical Engineering*, Vol. 56, No. 21, 231-240

[5] Pan, P. S. (2020). Design research of robot control system for automatic production line, *Machinery Design&Manufacture*, Vol. 2020, No. 4, 8-11, doi:10.19356/j.cnki.1001-3997.2020.04.003

[6] Marin-Martinez, F.; Campuzano-Bolarin, F.; Canas-Sanchez, H.; Mula, J. (2021). System dynamics model for flow time and lot sizes optimization according to Quick Response Manufacturing (QRM) strategy, *DYNA*, Vol. 96, No. 1, 105-111, doi:10.6036/9661

[7] Yang, L.; Qin, H.; Zhang, J.; Su, H.; Li, G.; Bai, S. (2021). Cloud model for security state recognition based on factor space, *IEEE Sensors Journal*, Vol. 21, No. 22, 25429-25436, doi:10.1109/JSEN.2021.3098679

[8] Grznar, P.; Gregor, M.; Gaso, M.; Gabajova, G.; Schickerle, M.; Burganova, N. (2021). Dynamic simulation tool for planning and optimisation of supply process, *International Journal of Simulation Modelling*, Vol. 20, No. 3, 441-452, doi:10.2507/IJSIMM20-3-552

[9] Sosa-Mendez, D.; Lugo-Gonzalez, E.; Arias-Montiel, M.; Garcia-Garcia, R. A. (2017). ADAMS-MATLAB co-simulation for kinematics, dynamics, and control of the Stewart-Gough platform, *International Journal of Advanced Robotic Systems*, Vol. 14, No. 4, 10 pages, doi:10.1177/1729881417719824

[10] Arreguin, J. L. R.; Ceccarelli, M.; Torres-SanMiguel, C. R. (2022). Design and simulation of a PK testbed for head impact evaluation, *Robotica*, Vol. 40, No. 5, 1293-1308, doi:10.1017/S0263574721001089

[11] Nidhi; Noble, S.; Sooraj, V. S. (2023). Bio-inspired skeletal model and kinematics of humanoid spine and ribs, *Proceedings of the Institution of Mechanical Engineers, Part C: Journal of Mechanical Engineering Science*, in press (Online First), doi:10.1177/09544062231166813

[12] Amiri, N.; Sohrabi, K.; Eftekharian, G.; Fakhari, V. (2023). Optimization and control of an energy-efficient vibration-driven robot, *Journal of Vibration and Control*, in press (Online First), 16 pages, doi:10.1177/10775463231175543

[13] Cretescu, N.; Neagoe, M.; Saulescu, R. (2023). Dynamic analysis of a delta parallel robot with flexible links and joint clearances, *Applied Sciences*, Vol. 13, No. 11, Paper 6693, 18 pages, doi:10.3390/app13116693

[14] John, I.; Mohan, S.; Rybak, L. (2022). Numerical investigations, development and control of a cartesian (3-PRRR) parallel manipulator, *Proceedings of the Institution of Mechanical Engineers, Part C: Journal of Mechanical Engineering Science*, Vol. 236, No. 15, 8635-8649, doi:10.1177/09544062221086856

[15] Satpute, N.; Jugulkar, L.; Jabade, S.; Korwar, G.; Arawade, S. (2022). Design and analysis of motion and energy regulating vibration harvester, *Proceedings of the Institution of Mechanical Engineers, Part C: Journal of Mechanical Engineering Science*, Vol. 236, No. 3, 1391-1405, doi:10.1177/09544062211021441
[16] Boomeri, V.; Tourajizadeh, H. (2020). Design, modelling, and control of a new manipulating climbing robot through infrastructures using adaptive force control method, *Robotica*, Vol. 38, No. 11, 2039-2059, doi:10.1017/S0263574719001814
[17] Thomas, M. J.; Joy, M. L.; Sudheer, A. P. (2020). Kinematic and dynamic analysis of a 3-PRUS spatial parallel manipulator, *Chinese Journal of Mechanical Engineering*, Vol. 33, Paper 13, 17 pages, doi:10.1186/s10033-020-0433-8
[18] Karamipour, E.; Dehkordi, S. F.; Korayem, M. H. (2020). Reconfigurable mobile robot with adjustable width and length: conceptual design, motion equations and simulation, *Journal of Intelligent & Robotic Systems*, Vol. 99, No. 3-4, 797-814, doi:10.1007/s10846-020-01163-7
[19] Chen,Y.-D.; Dai, B.-Y.; Feng, X. (2017). Simulation and analysis of the working device of gripping machine based on UG and STEP function, *Equipment Manufacturing Technology*, Vol. 2017, No. 12, 76-78
[20] Liu, J. H.; Shi, Y. P.; Yu, L. T.; Li, J.; Yuan, J. (2022). Research on motion simulation of virtual model of stamping machine based on ADAMS, *Modern Manufacturing Technology and Equipment*, Vol. 2022, No. 3, 107-109, doi:10.16107/j.cnki.mmte.2022.0189
[21] Liu, Y.-C.; Hu, Y.-C.; Peng, S.-X. (2019). Kinematics simulation analysis of rocker type mullberry leaf picking device, *Equipment Manufacturing Technology*, Vol. 2019, No. 12, 1-4
[22] Zhao, S.-T.; Fu, Y.-Y.; Lu, Q.; Zheng, Q. (2020). Research on the modelling and kinematics simulation of globoidal indexing cam mechanism based on Creo and ADAMS, *Machinery Design & Manufacture*, Vol. 2020, No. 4, 111-114, doi:10.19356/j.cnki.1001-3997.2020.04.027
[23] Ma, Q.; Chen, Z.; Zhang, X. C.; Hu, X. (2013). Motion simulation analysis of harvesting robot arm based on ADAMS, *Journal of Agricultural Mechanization Research*, Vol. 2013, No. 5, 37-40, doi:10.13427/j.cnki.njyi.2013.05.015
[24] Liu, X.; Jian, Z.; Ding, Z. J.; Zhang, Y. (2021). Gait planning and motion simulation of lower limb prosthesis based on CPG, *Machine Tool & Hydraulics*, Vol. 49, No. 18, 135-138